NJC

Accepted Manuscript

This article can be cited before page numbers have been issued, to do this please use: A. Jehdaramarn, S. Pornsuwan, P. Chumsaeng, K. Phomphrai and P. Sangtrirutnugul, *New J. Chem.*, 2017, DOI: 10.1039/C7NJ03113K.

View Article Online
DOI: 10.1039/C7NJ03113K

Effects of Appended Hydroxyl Groups and Ligand Chain Length on Copper Coordination and Oxidation Activity

Attawit Jehdaramarn,[†,‡] Soraya Pornsuwan,[†] Phongnarin Chumsaeng,[†,§]

Khamphee Phomphrai,[§] and Preeyanuch Sangtrirutnugul[†,‡,*]

* Corresponding author. Email: preeyanuch.san@mahidol.ac.th

[†]Center of Excellence for Innovation in Chemistry (PERCH-CIC), Department of Chemistry, Faculty of Science, Mahidol University, 272 Rama VI Rd. Bangkok, 10400, Thailand.

[‡]Center for Catalysis, Department of Chemistry, Faculty of Science, Mahidol University, 272 Rama VI Rd. Bangkok, 10400, Thailand.

[§]Department of Materials Science and Engineering, School of Molecular Science and Engineering, Vidyasirimedhi Institute of Science and Technology, Rayong, 21210, Thailand

Abstract

Treatment of a series of (imino)pyridine ligands bearing appended hydroxyl groups 2-((pyridin-2-ylmethylene)amino)phenol (Hpyph), 2-((pyridin-2-ylmethylene)amino)-ethanol (Hpyet), and 3-((pyridin-2-ylmethylene)amino)propanol (Hpypr) with one equiv of $CuCl_2$•$2H_2O$ afforded the corresponding Cu(II) complexes in low to moderate yields. The crystal structure of $(\mu\text{-Cl})_2[CuCl(\kappa^2\text{-}N,N\text{-Hpyet})]_2$ reveals a symmetric dinuclear structure with the bidentate N,N coordination mode of (imino)pyridine with no Cu--OH interaction. On the other hand, the dinuclear Cu(II) complex of the related propyl ligand Hpypr possesses a significantly different crystal structure involving nucleophilic addition of the hydroxyl group to the aldehyde group of 2-pyridinecarboxaldehyde. The catalyst system Cu complex/Cu^0/TEMPO/Na_2CO_3 (TEMPO = 2,2,6,6-tetramethylpiperidinyl-1-oxyl) generally exhibited good activities for aerobic oxidation of benzyl alcohol to benzaldehyde in H_2O at room temperature. The dinuclear Cu(II) complex $(\mu\text{-Cl})_2[CuCl(\kappa^2\text{-}N,N\text{-Hpyet})]_2$ was demonstrated as an effective catalyst toward aerobic oxidation of various benzyl alcohol derivatives, cinnamyl alcohol, and 2-thiophenemethanol.

View Article Online
DOI: 10.1039/C7NJ03113K

Keywords: Appended hydroxyl group, copper catalyst, aerobic alcohol oxidation, water soluble catalyst

Introduction

Copper-catalyzed oxidation of alcohols to the corresponding aldehydes using oxygen or air as an oxidant is generally highly efficient and can be performed under environmentally friendly conditions.[1] Sammelhack and co-workers first reported the catalyst system CuCl/TEMPO/DMF (TEMPO = 2,2,6,6-tetramethylpiperidinyl-1-oxyl, DMF = *N*,*N*-dimethylformamide), which were effective for oxidation of primary alcohols to aldehydes under an atmospheric O_2.[2] Later works by Sheldon,[3] Koshinen,[4] and Stahl[5] involved copper catalyst systems supported by 2,2'-bipyridine ligand in the presence of an additional base including KO^{t}Bu, 1,8-diazabicyclo[5.4.0]undec-7-ene (DBU), and *N*-methylimidazole (NMI) with O_2 or ambient air as an oxidant in CH_3CN. Other related N-based ligands have also been investigated as catalyst supports by our group and others.[6-9] For environmental reasons, there have recently been a growing interest in copper-catalyzed aerobic alcohol oxidation in water. Zhang[9] and Rheingold[10] reported water-soluble copper catalysts supported by N-based ligands, which were active toward aerobic oxidation of benzyl alcohols in water. Lipshutz[11] also demonstrated that the designer surfactant TPGS-750-M was effective at facilitating Cu-catalyzed aerobic alcohol oxidation in an aqueous solution (Table 1).

Notably, active copper species for aerobic oxidation of alcohols is a key component in the enzyme Galactose Oxidase (GOase).[12] The distorted square pyramidal copper(II) active site in GOase consists of two nitrogen donors from two histidine imidazoles and, at the axial position, a phenol group of tyrosine, which facilitates oxidative transformation.[13, 14] Further evidences for the role of hydroxyl group in oxidation were reported by Puddephatt and co-workers, in which appended phenol and hydroxyethyl groups in the ligand framework were shown to promote reactions between a dimethylplatinum(II) complex and O_2.[15, 16] Despite these findings, no related studies have been carried out on molecular copper catalyst systems. Based on established oxidation activities of copper catalysts and potential involvement of appended hydroxyl groups in metal-catalyzed oxidation, we prepared multidentate ligands featuring N,N,O donors from pyridine, Schiff base, and hydroxyl groups with three different ligand backbones. The corresponding Cu(II) complexes were used as

View Article Online
DOI: 10.1039/C7NJ03113K

catalysts for aerobic alcohol oxidation in an alkaline aqueous solution and their catalytic activities were compared. In particular, this work aims to evaluate the effects of appended hydroxyl groups associated with ligand rigidity and chain length on the coordination environments at the Cu(II) center and their subsequent catalytic activities toward oxidation reactions.

Table 1. Known Cu catalyst systems for aerobic oxidation of benzyl alcohol in water

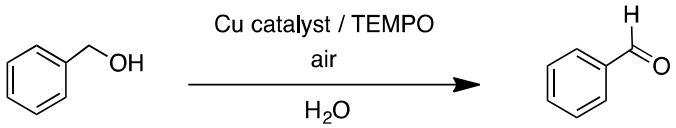

Cu catalyst	Solvent	Temp. (^oC)	Ref.
$Cu(OAc)_2•H_2O$/pytl-β-CD/Na_2CO_3	H_2O	100	9
$(\mu\text{-}Cl)_2[Cu(bzm)Cl]_2$	H_2O	RT	10
CuBr/bpy/NMI	2 wt% TPGS-750-M in H_2O	RT	11

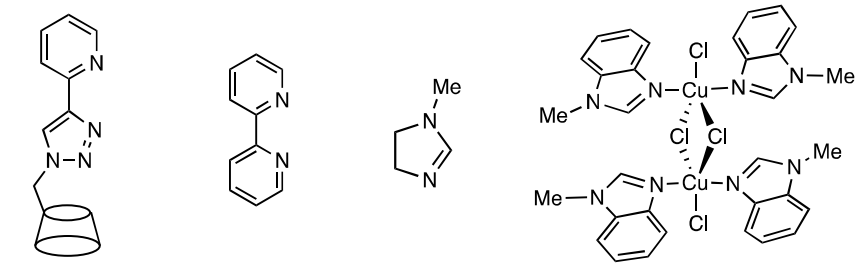

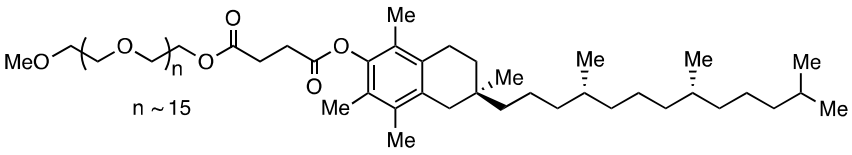

TPGS-750-M

Experimental Section

Materials. 2-Pyridinecarboxaldehyde, 2-aminophenol, 2-aminoethanol, and 3-aminopropanol (Aldrich) were of reagent grade and used as received. The commercial grade ethyl acetate, dichloromethane, and hexane were distilled prior to use. All other

View Article Online
DOI: 10.1039/C7NJ03113K

chemicals and solvents used in this work are of reagent or analytical grade and were used as received.

Physical Measurements. Fourier transform nuclear magnetic resonance spectra were recorded by a Bruker's Ascend 400 high-resolution magnetic resonance spectrometer. Chemical shifts were reported in δ units (parts per million) using residual solvents peaks as references. Mass spectrometric analysis was carried out using a Bruker micro TOF spectrometer in the ESI mode whereas elemental analyses were performed on a Perkin Elmer 2400 CHN. Fourier transform infrared spectroscopy (FTIR) were collected on Bruker Alpha instrument (Bruker Optics GmbH, Ettlingen, Germany) (400–4000 cm^{-1}). UV-visible spectra of the aqueous solutions of the Cu(II) complexes **1**–**3** were obtained from JASCO model V-530 and recorded in the range 200–800 nm. Powder X-ray diffraction (PXRD) was performed by Bruker AXS model D8 Discover with a monochromatic Cu K_α (40 kV, 40 mA) source with a step size of 0.020^o and a step time of 0.2 $s \bullet step^{-1}$. The electron spin resonance (ESR) spectra were obtained at room temperature using a Bruker Elexys500 X-band spectrometer. The solid powder samples were packed in 1.5 mm OD capillary tubes. All measurements were performed at a frequency of ~9.8 GHz and microwave power of 2 mW. The center field was set at 3200 G with 1500 G sweep width and the modulation amplitude was at 4 G. Single crystal X-ray analyses of the complexes **2** and **3** were carried out at VISTEC. The X-ray crystallographic data were collected at low temperatures on a Bruker D8 venture using Photon II detector and IμS 3.0 Microfocus source, Mo K_α radiation (λ = 0.71073 Å). Data integration was performed using *SAINT* and intensity data were corrected based on the intensities symmetry-related reflections measured at different angular setting (*SADABS*). The space group were determined using *XPREP* whereas the structure was solved by intrinsic phasing method (*XT* program) and refined by full-matrix least squares against F^2 using the *XL* program based on *ShelXle* engine. Product yields and percent substrate conversions obtained from catalytic experiments were analyzed by GLC on a 6890N Agilent Technologies gas chromatograph equipped with a 5973N Agilent Technologies quadrupole mass detector.

Synthesis of the Schiff base ligands. To a 40 mL EtOH solution of 2-pyridinecarboxaldehyde (950 μL, 10 mmol) was added aminoalcohol (10 mmol). The

View Article Online
DOI: 10.1039/C7NJ03113K

reaction mixture was refluxed for a certain amount of time, after which all volatiles were removed under vacuum.

2-((Pyridin-2-ylmethylene)amino)phenol (Hpyph). 2-Aminophenol (1.09 g, 10 mmol) was used. The mixture was refluxed for 1 h. Crystallization from slow evaporation of diethyl ether solution gave a yellow powder in 60% yield (1.190 g, 6.0 mmol). ^{1}H NMR (400 MHz, DMSO-d_6): δ 9.23 (s, 1 H, ArO*H*), 8.71 (s, 1 H, =N*H*), 8.69 (m, 1 H, Ar*H*), 8.38 (d *J* = 8 Hz, 1 H, Ar*H*), 7.94 (t *J* = 8 Hz, 1 H, Ar*H*), 7.50 (m, 1 H, Ar*H*), 7.29 (m, 1 H, Ar*H*), 6.92 (d *J* = 8 Hz, 1 H, Ar*H*), 6.85 (m, 1 H, Ar*H*). ^{13}C{^{1}H} NMR (100 MHz, DMSO-d_6): δ 159.4, 154.5, 151.4, 149.5, 136.8, 128.3, 125.4, 121.5, 119.7, 119.6, 116.3, 114.4 (aromatic *C*s). FT-IR (cm^{-1}): 3378 (br, O–H), 1628 (C=N), 1151 (C–OH).

2-((Pyridin-2-ylmethylene)amino)ethanol (Hpyet). 2-Aminoethanol (600 μL, 10 mmol) was used. The mixture was refluxed for 24 h. Solvent evaporation under reduced pressure gave yellow oil in 93% yield (1.40 g, 9.3 mmol). The product was pure based on the ^{1}H NMR spectrum and was used in the next step without further purifications. ^{1}H NMR (400 MHz, DMSO-d_6): δ 8.63 (m, 1 H, py*H*), 8.31 (s, 1 H, =N*H*), 7.96 (m, 1 H, py*H*), 7.87 (m, 1 H, py*H*), 7.46 (m, 1 H, py*H*), 4.65 (br s, 1 H, O*H*), 3.68 (br s, 4 H, CH_2CH_2). ^{13}C{^{1}H} NMR (100 MHz, DMSO-d_6): δ 162.7, 154.2, 149.3, 136.8, 125.0, 120.4 (aromatic *C*s), 63.1 60.5 (*C*H$_2$*C*H$_2$). FT-IR (cm^{-1}): 3278 (br, O–H), 1649 (C=N), 1059 (C–OH).

3-((Pyridin-2-ylmethylene)amino)propanol [Hpypr (a)] and tetrahydro-2-(2-pyridinyl)-2*H*-1,3-oxazine [Hpypr (b)]. 3-Aminopropanol (765 μL, 10 mmol) was used. The reaction mixture was refluxed for 24 h. Solvent evaporation under reduced pressure gave yellow oil (1.51 g). A mixture of open chain form and cyclic form was obtained in *ca*. 8:1 ratio.

Hpypr (a): ^{1}H NMR (400 MHz, DMSO-d_6): δ 8.63 (d *J* = 4 Hz, 1 H, Ar*H*), 8.34 (s, 1 H, =N*H*), 7.94 (d *J* = 8 Hz, 1 H, Ar*H*), 7.86 (dt *J* = 8, 2 Hz, 1 H, Ar*H*), 7.45 (m, 1 H, Ar*H*), 4.50 (t *J* = 5 Hz, 1 H, O*H*), 3.68 (dt *J* = 8, 1 Hz, 2 H, =NCH_2), 3.48 (m, 2 H, CH_2OH), 1.78 (quin *J* = 6 Hz, 2 H, CH_2). ^{13}C{^{1}H} NMR (100 MHz, DMSO-d_6): δ 161.8, 154.2, 149.3, 136.8, 125.0, 120.4 (aromatic *C*s), 58.5, 57.2, 33.6 (*C*H$_2$*C*H$_2$*C*H$_2$).

Hpypr (b): ^{1}H NMR (400 MHz, DMSO-d_6): δ 8.50 (d *J* = 4 Hz, 1 H, Ar*H*), 8.34 (s, 1 H, =N*H*), 7.79 (dt J = 8, 2 Hz, 1 H, Ar*H*), 7.32 (m, 1 H, Ar*H*), 5.06 (s, 1 H, pyC*H*),

View Article Online
DOI: 10.1039/C7NJ03113K

1.31–4.09 (m, 6 H, C*H*$_2$). ^{13}C{^{1}H} NMR (100 MHz, DMSO-d_6): δ 148.5, 136.7, 123.4, 121.2 (aromatic *C*s), 89.6 (py*C*H), 67.3, 43.6, 26.5 (*C*H$_2$*C*H$_2$*C*H$_2$). FT-IR (cm^{-1}): 3285 (br, O–H), 1649 (str, C=N), 1058 (str, C–OH).

Synthesis of the Cu(II) complexes (1–3). A equimolar mixture of $CuCl_2$•$2H_2O$ and ligands **1**–**3** was stirred in 40 mL of CH_2Cl_2 at room temperature for 24 h. All volatiles were then removed *in vacuo* and the remaining solids were crystallized from suitable solvents.

[2-((Pyridin-2-ylmethylene)amino)phenol]copper(II) Chloride (1). Hpyph (0.22 g, 1.1 mmol) and $CuCl_2$•$2H_2O$ (0.20 g, 1.1 mmol) were used. Crystallization from slow evaporation of the CH_3CN solution afforded brown powder in 46% yield (0.17 g, 0.51 mmol). FT-IR (cm^{-1}): 3432 (br, O–H), 1648 (C=N).

[2-((Pyridin-2-ylmethylene)amino)ethanol]copper(II) Chloride (2). Hpyet (0.20 g, 1.3 mmol) and $CuCl_2$•$2H_2O$ (0.22 g, 1.3 mmol) were used. A layer diffusion of Et_2O onto the DMF solution of **2** at room temperature afforded a green microcrystalline solid in 35% yield (0.27 g, 0.46 mmol). Anal. Calcd. for $C_{16}H_{20}N_4O_2Cu_2Cl_4$: C, 33.76; H, 3.54; N, 9.84 Found: C, 33.56; H, 3.53; N, 9.95. FT-IR (cm^{-1}): 3430 (br, O–H), 1648 (C=N), 1058 (C–OH).

[3-((Pyridin-2-ylmethylene)amino)propanol]copper(II) Chloride (3). Hpypr (0.20 g, 1.2 mol) and $CuCl_2$•$2H_2O$ (0.21 g, 1.2 mol) were used. A layer diffusion of EtOAc onto the DMF solution of **3** at room temperature afforded a green microcrystalline solid in 30% yield (0.18 g, 0.36 mmol). Anal. Calcd. for $C_{15}H_{16}N_3O_2Cu_2Cl_3$: C, 35.76; H, 3.20; N, 8.34 Found: C, 36.13; H, 3.04; N, 8.21. FT-IR (cm^{-1}): 1607 (C=N), 1042 (C–O–C).

General procedure for alcohol oxidation

To a 3 mL of an aqueous solution of the Cu(II) complex (0.050 mmol Cu) and Cu^0 sheets (a total surface area = 1.0 cm^2) was added 1.0 mmol of alcohol. To ensure the same concentration of the Cu active species, 0.050 mmol Cu was calculated based on 0.025 mmol of the dinuclear copper complexes **1**–**3**. A 2 mL aqueous solution of TEMPO (0.050 mmol) and Na_2CO_3 (0.10 mmol) was added and the reaction mixture was stirred in air at room temperature for a given time. Then, the aqueous solution was extracted with 3x10 mL of CH_2Cl_2. The combined organic layers were dried using anhydrous Na_2SO_4 and filtered, after which the solvent was removed. The

View Article Online
DOI: 10.1039/C7NJ03113K

percent conversions were quantified using the GC-MS method, in which EtOAc was used as a solvent in the presence of anisole (0.10 mmol) as the internal standard.

Results and Discussion

Synthesis of Ligands and the Cu(II) Complexes.

The (imino)pyridine ligands Hpyph, Hpyet, Hpypr were prepared according to previous literatures,[17, 18] with slight modifications *via* condensation of 2-pyridinecarboxaldehyde and their respective aminoalcohols in EtOH under refluxed conditions (Scheme 1). The phenylene-containing product Hpyph appeared as a yellow solid which was purified and isolated in 60% yield by crystallization in diethyl ether. Meanwhile, ligands with an alkyl framework Hpyet and Hpypr were obtained as yellow oils. Based on their ^{1}H NMR spectra in DMSO-d_6, the ethylene linker Hpyet exists only in an open chain form whereas the propyl derivative Hpypr is in equilibrium between the open chain (**a**) and the cyclic (**b**) forms. The ^{1}H NMR integration reveals that the crude product of Hpypr has the open chain form as a major species (*ca.* 8:1 ratio of (**a**):(**b**) in DMSO-d_6, Figure S5). On the contrary, Puddephatt *et. al.*, whose work was published during the course of our study, reported the cyclic form of Hpypr (**b**) as a dominant product (*ca*. 80%) in $CDCl_3$ solution.[16]

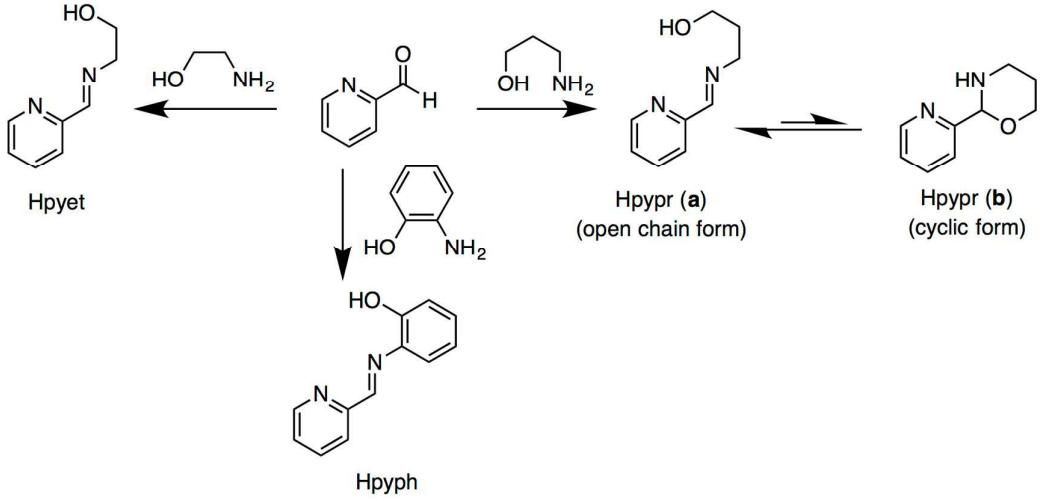

Scheme 1. Ligand synthesis

Treatments of $CuCl_2$•$2H_2O$ with an equimolar of Hpyph in CH_2Cl_2 at room temperature for 24 h resulted in a brown solid, while, under the same conditions, reactions with Hpyet or Hpypr gave green crystals (Scheme 2). The phenylene-containing Cu(II) complex **1** was isolated *via* slow evaporation of the CH_3OH solution at room temperature, which afforded a brown crystalline solid in 46% yield.

View Article Online
DOI: 10.1039/C7NJ03113K

Attempts to obtain a solid state structure of **1** have so far been unsuccessful. On the other hand, layering the DMF solutions of Cu(II) complexes **2** and **3** with Et_2O (for **2**) or EtOAc (for **3**) at room temperature gave green crystalline solids suitable for X-ray analysis in 35% and 30% yields, respectively. The FT-IR spectra of **1** and **2** contain a broad absorption band at *ca*. 3430 cm^{-1} whereas no absorption band corresponding to O–H stretching was observed in that of **3** (Figure S8, S10, and S12). Furthermore, the powder XRD analyses of **2** and **3**, both from the crude samples and the isolated crystalline solids, reveal the same XRD patterns confirming that the obtained crystals represent the major products from Cu complexation (Figure S14 and S15). It should be noted that Pal and co-workers have previously reported the synthesis and crystal structure of Cu(pyph)Cl, generated from a similar reaction of Hpyph with $CuCl_2 \bullet 2H_2O$ and KOH in refluxing CH_3OH.[17] For our experiment, even in the absence of a base, it is possible that the acidic phenolic proton may be deprotonated. To gain insights into the structure of **1**, the powder XRD spectrum of the isolated complex **1** and that simulated from single crystal data of Cu(pyph)Cl were compared, showing different XRD patterns (Figure S13). On the basis of powder XRD results and the presence of OH absorption band in the FT-IR spectrum, the dimeric structure similar to that of **2** is proposed for the phenylene derivative **1** (Scheme 2 and Figure 1).

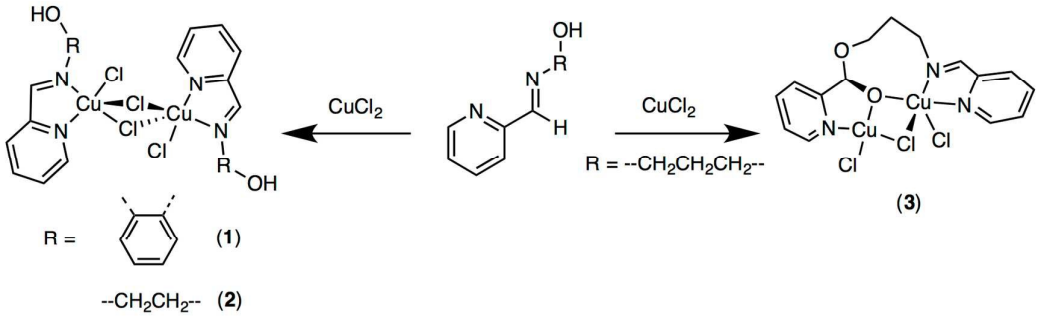

Scheme 2. Synthesis of Cu(II) complexes **1**–**3**.

Structure description of complexes 2 and 3

X-ray data of **2** reveal a chloride-bridged asymmetric dinuclear Cu(II) complex with a square pyramidal geometry at the copper center ($\tau = 0.06$, where $\tau = 0$ for a square pyramid and $\tau = 1$ for a trigonal bipyramid),[19] as shown in Figure 1. The Cu(1) and Cu(1A) ions are related by inversion and each copper center is chelated by

View Article Online
DOI: 10.1039/C7NJ03113K

pyridine and imine N donors, both of which are at basal sites. A terminal Cl and a bridging Cl ion complete basal positions whereas another bridging Cl locates at the axial position. The bite angle $N_{py}(2)$–Cu(1)–$N_{im}(1)$ is small at 80.26(4)^o whereas the bond distances of Cu(1)–$N_{py}(2)$ (2.030(1) Å) and Cu(1)–$N_{im}(1)$ (2.032(1) Å) are closely similar. The terminal Cu(1)–Cl(2) and bridging Cu(1)–Cl(1) bond distances at basal sites are 2.2833(6) and 2.2679(6) Å, respectively, which are considerably shorter than that of the bridging, axial Cu(1)–Cl(1A) bond (2.791(1) Å). Furthermore, through bridging Cl ligands, the intramolecular Cu---Cu separation is 3.647(1) Å, comparable to other related dinuclear complexes with the Cu(μ-Cl)$_2$Cu core.[20, 21] It is worth mentioning that Puddephatt and co-workers have recently reported results from DFT calculations of the related complexes Pt(L)Me$_2$ (L = Hpyet and Hpypr).[16] The calculations suggest that the stable conformations involve a hydroxyl substituent directing toward the Pt(II) center and forming a weak hydrogen bond. On the contrary, the related crystal structure of the Cu(II) complex **2** exhibits no apparent Cu--OH interactions.

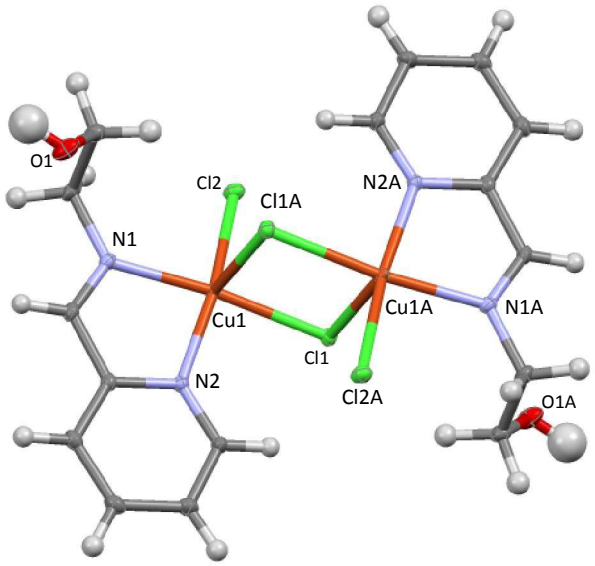

Figure 1. The ORTEP representation of **2** with thermal ellipsoid at the 50% probability. Selected bond parameters: Cu1–N1 = 2.032(1), Cu1–N2 = 2.030(1), Cu1–Cl1 = 2.2833(6), Cu1–Cl2 = 2.2679(6), Cu1–Cl1A = 2.791(1) Å; N1–Cu1–N2 = 80.26(3), Cl1–Cu1–Cl2 = 92.06(1), N1–Cu1–Cl1 = 173.07(3), N2–Cu1–Cl2 = 169.55(3), Cl1–Cu1–Cl1A = 88.33(1)^o.

Unlike **2**, the solid state structure of **3** reveals an unsymmetric dinuclear Cu(II) complexes, featuring five coordinate Cu1 and four coordinate Cu2 (Figure 2).

View Article Online
DOI: 10.1039/C7NJ03113K

Both Cu1 and Cu2 ions are bridged by the oxygen atom O2 of the alkoxy group and a chloride ion. The bridging Cu1–O2–Cu2 bond angle is 110.96(9)°. The Cu1 ion has a distorted square pyramidal geometry based on has the τ value[19] of 0.26 and is supported by a tridentate N,N,O ligand, a terminal Cl, and a bridging Cl ion. On the other hand, the Cu2 ion possesses a distorted square planar geometry and is surrounded by the bidentate N,O ligand with the bite angle O2–Cu2–N3 of 81.73(9)°, a terminal Cl, and a bridging Cl. The sum of six independent angles at Cu2 is *ca*. 703°, significantly deviated from the expected 720° for the square planar structure. Interestingly, the Cu---Cu separation in **3** is 3.199(2) Å, which is significantly shorter than that in **2**. In addition, despite the presence of chiral centers such as Cu1 and C10 atoms in the molecule, only one diastereomer crystallized from a mixture of DMF:EtOAc solvent.

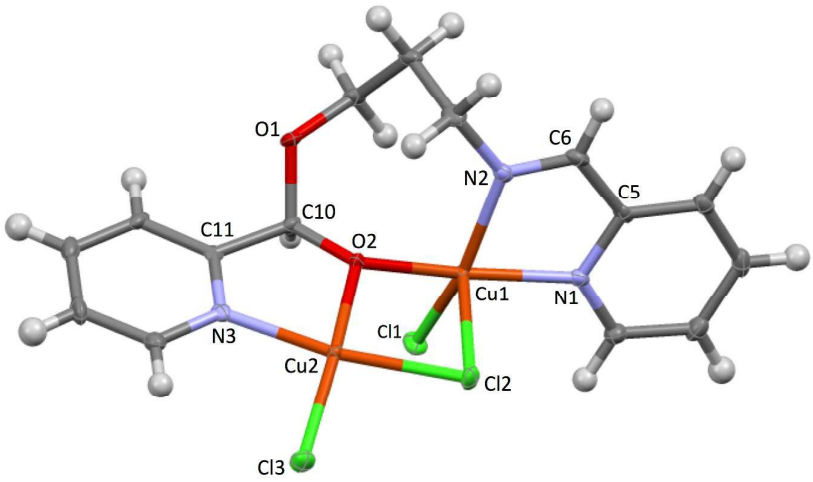

Figure 2. The ORTEP representation of **3** with thermal ellipsoid at the 50% probability. Selected bond parameters: Cu1–N1 = 2.007(3), Cu1–N2 = 2.004(3), Cu1–O2 = 1.962(2), Cu2–O2 = 1.920(2), Cu2–N3 = 2.004(3), Cu1–Cl1 = 2.242(1), Cu1–Cl2 = 2.591(2), Cu2–Cl2 = 2.275(1), Cu2–Cl3 = 2.209(1) Å; N1–Cu1–N2 = 80.8(1), Cl1–Cu1–O2 = 94.67(6), Cl2–Cu1–O2 = 77.08(6), O2–Cu1–N2 = 91.04(9), Cl2–Cu2–Cl3 = 96.36(3), O2–Cu2–N3 = 81.73(9), Cl2–Cu2–O2 = 86.22(6), N3–Cu2–Cl3 = 95.57(7), Cu1–O2–Cu2 = 110.96(9), Cu1–Cl2–Cu2 = 81.92(3)°.

For the (imino)pyridine ligands, the coordination behaviors of the appended hydroxyl group are rather unexpected. The related NNO and ONO ligand systems featuring an appended alcohol functional group have been crystallographically characterized or proposed as tridentate ligands with M--OH interactions.[16, 18, 22, 23] In contrast, our results have revealed no Cu--OH interaction in the solid state structure,

View Article Online
DOI: 10.1039/C7NJ03113K

for the ethylene-based ligand. Furthermore, for the slightly longer propylene linker, the intermolecular nucleophilic addition of OH group was evident according to the crystal structure. In particular, formation of the dinuclear Cu(II) complex **6** is likely a result of Cu-catalyzed imine hydrolysis to generate Cu-coordinated 2-pyridinecarboxaldehyde followed by nucleophilic addition of the appended propyl alcohol at the aldehyde group. Several works have previously documented copper-promoted hydrolysis of the Schiff base ligands to generate the constituent aldehyde and amine precursors.[24, 25] Hammershøi and Cuevas also independently demonstrated that the coordinated imine ligands were susceptible to nucleophilic attacks.[26-28] However, to the best of our knowledge, Cu-catalyzed imine hydrolysis followed by nucleophilic addition at aldehyde to afford the 8-membered dinuclear metallacycle is unprecedented.

The effect of linker chain length of pyridine-diimine-based ligands on complex's stability has been previously investigated by Ghosh and co-workers. It was found that while the Cu(II) complex of the ethylene-linked pyridine-diimine ligand was stable, the related propylene-linked ligand underwent hydrolysis and rearrangement in the presence of Cu(II) or H^+ ion.[25] Lower stability of the propylene-based chelate ligand was attributed to more steric strain, as a result of two adjacent six-membered metallacyclic rings. However, in this work, since the hydroxyl groups of the (imino)pyridine ligands do not coordinate to the Cu(II) centers, we reason that the drastic differences in the ligand activity stems from the alkyl chain length. In particular, the longer alkyl chain of the propyl alcohol enables the hydroxyl group to reach farther away from the Cu coordination sphere for subsequent nucleophilic addition.

Spectroscopic and ESR study.

UV-vis spectra of the Cu(II) complexes in DMSO contain a weak absorption band at 447, 709, and 714 cm^{-1} assignable to Cu(II) *d-d* transitions for **1**, **2**, and **3**, respectively (Figure S16–S18). Meanwhile, intense absorption bands between 200–350 cm^{-1} were attributed to π-π* transition (intraligand) and ligand-to-metal charge transfer.[29, 30] The ESR powder spectra of **1**–**3** contain the two signals, $g_\perp$ and $g_\parallel$, as illustrated in Figure 3. Table 2 shows the magnetic parameters for the g-values of each Cu complex. The elongated axial symmetry characterized by $g_\parallel > g_\perp > 2.0023$ is

View Article Online
DOI: 10.1039/C7NJ03113K

consistent with distorted square pyramid and square planar geometry at Cu(II) ions, as confirmed by the solid state structures of **2** and **3** (*vide supra*).[31] The g-value parameters obtained from **1**–**3** are comparable to our previously reported ESR data for the mononuclear distorted square planar complex of the type (NN')$CuCl_2$ ($g_\perp$ ~ 2.07–2.08 and $g_\parallel$ ~ 2.25–2.28),[7] suggesting weak exchange interactions between copper ions in the dinuclear Cu complexes. Another interesting feature of these ESR data is a significantly smaller separation between $g_\perp$ and $g_\parallel$ for **3** (Δg = 0.125 compared to 0.204 (for **1**) and 0.188 (for **2**); Table 2). The lowering in Δg value is attributed to a stronger interaction at the d^9 Cu electron, as a result of a bridging paramagnetic O donor compared to a bridging Cl atom (Figure 1 and 2). Furthermore, based on the closely related g-value parameters of **1** and **2** together with their FT-IR and powder XRD data, we propose that the solid state structure of **1** possesses similar coordination environment to that of **2** (*vide supra*).

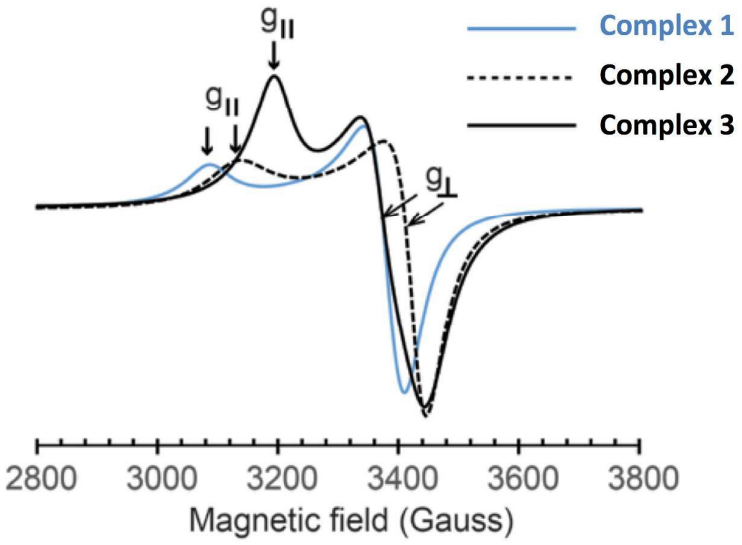

Figure 3. ESR powder spectra of the Cu complexes **1**–**3** at room temperature. The *g*-values of each complexes were shown as $g_\perp$ and $g_\parallel$ indicated in arrow signs.

Table 2. Magnetic parameters obtained from the ESR spectra of **1**–**3** in solid powder.

Cu complex	$g_\perp$	$g_\parallel$	Δg*
1	2.091	2.295	0.204
2	2.068	2.256	0.188
3	2.091	2.216	0.125

View Article Online
DOI: 10.1039/C7NJ03113K

* Δg is calculated by $g_{\parallel} - g_{\perp}$.

Aerobic alcohol oxidation in water

The Cu(II) complexes **1**–**3** were investigated as catalysts for aerobic alcohol oxidation in an aqueous solution. First, the catalytic activities of **1**–**3** were compared using 1.0 mmol of benzyl alcohol as the model substrate, catalyzed by 5 mol% Cu(II) species, 5 mol% TEMPO, Cu^0 sheets with a total area of 1 cm^2, and 10 mol% Na_2CO_3 under air at room temperature with the H_2O solvent (Table 3). In comparison, the activities of **2** and **3** are comparable, giving benzaldehyde as a sole product in excellent conversions after 16 h, and higher than that of **1** (entries 1–3). Interestingly, different coordination environments at the Cu centers in the dinuclear Cu(II) complexes **2** and **3** did not have a significant impact on oxidation activities. The reduced catalytic activities of **1** was explained by a decrease in the electron density at the copper center as a result of the more electron-withdrawing phenylene groups.[32] Next, the effect of base was investigated using the catalyst **2**. Under similar conditions, 10 mol% of Na_2CO_3 at room temperature furnished a near quantitative conversion of benzyl alcohol to benzaldehyde whereas other bases including Cs_2CO_3, K_3PO_4, and *N*-methylimidazole (NMI) resulted in lower conversions (entries 4–6). Decreased conversions were also obtained with reduced catalyst loadings (from 5 mol% to 1 mol% Cu), the use of $CuCl_2$ with no ligand, and the *in situ* generated Cu(II) complex (entries 7–9). Similarly, lower conversions were observed with the catalyst systems in the absence of either Cu^0 sheets (75%, entry 10) or Cu(II) catalyst (18%, entry 11). These results suggest that the most effective catalyst system requires both Cu(II) species and Cu^0 to undergo a comproportionation reaction[33, 34] and generate the Cu(I) species, which are more active toward catalytic oxidation.[35]

View Article Online
DOI: 10.1039/C7NJ03113K

Table 3. Catalyst comparison for aerobic alcohol oxidation[a]

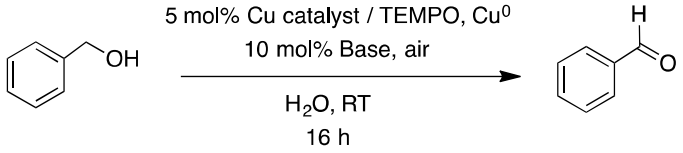

Entry	Cu catalyst	Base	Conversion (%)[b]
1[c]	**1**	Na_2CO_3	83
2	**2**	Na_2CO_3	93
3	**3**	Na_2CO_3	94
4	**2**	Cs_2CO_3	84
5	**2**	K_3PO_4	58
6[c]	**2**	NMI	87
7[d]	**2**	Na_2CO_3	86
8	$CuCl_2$	Na_2CO_3	37
9	$CuCl_2$/Hpyet	Na_2CO_3	62
10[e]	**2**	Na_2CO_3	75
11	-	Na_2CO_3	18

[a] Reaction Conditions: Benzyl alcohol (1.0 mmol), Cu catalyst (5 mol% based on Cu), TEMPO (0.050 mmol), base (0.10 mmol), four Cu^0 sheets with a total area of 1 cm^2 in H_2O (5 mL) under aerobic conditions with 0.010 mmol of anisole as an internal standard, room temperature, 16 h. [b] Determined by GC-MS. [c] Reaction time = 24 h. [d] The catalyst loading = 1 mol% of **2**. [e] Without Cu^0 sheet.

To investigate the substrate scope, the catalyst **2** was selected for further studies. Aerobic oxidation of benzylic alcohol derivatives were evaluated as shown in Table 4. Electron-donating OMe and OH groups generally gave good to excellent conversions after 16 h at room temperature (entries 1–3). On the other hand, the electron-withdrawing NO_2 group on benzyl alcohol afforded slower reactions as only moderate conversions were observed after 48 h (entries 4 and 5). Halogen-substituted benzyl alcohols gave mixed results: 4-iodobenzyl alcohol was completely converted to the oxidized product after 16 h whereas 4-bromo and 4-chlorobenzyl alcohols needed 48 h to reach high conversions (87% and 93%, respectively; entries 6–8). Cinnamyl alcohol was oxidized to the corresponding aldehyde in a quantitative conversion after 8 h (entry 9). Sulfur atom in 2-thiophenemethanol is well tolerated

View Article Online
DOI: 10.1039/C7NJ03113K

giving a complete conversion after 24 h (entry 10). Attempts to oxidize aliphatic primary and secondary alcohols including cyclohexane, 1-hexanol, 2-methyl-1-pentanol under similar catalytic conditions at room temperature and at 100 °C were unsuccessful.

Table 4. Substrate scope study[a]

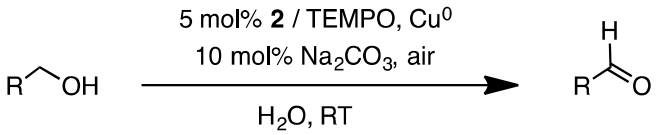

Entry	aldehyde	Time (h)	Conversion (%)[b]
1	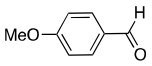	16	>99
2	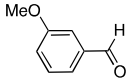	16	69
3	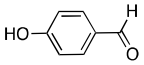	16	>99
4	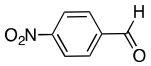	48	42
5	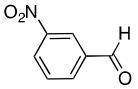	48	51
6	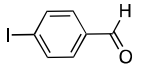	16	>99
7	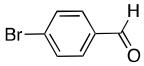	16	59 (87)[c]
8	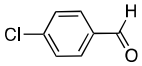	16	58 (93)[c]
9	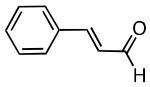	8	>99
10	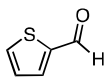	16	76 (>99)[d]

[a] Reaction Conditions: Alcohol substrate (1.0 mmol), Cu complex **2** (0.025 mmol), TEMPO (0.050 mmol), Na_2CO_3 (0.10 mmol), four Cu^0 sheets with a total area of 1 cm^2 in H_2O (5 mL) under aerobic conditions at room temperature with 0.010 mmol of anisole as an internal standard. [b] Based on GC analysis. Since the corresponding aldehyde is the only product

View Article Online
DOI: 10.1039/C7NJ03113K

observed, % conversion = the ratio of product x 100/(product + starting material). [c] Reaction time = 48 h. [d] Reaction time = 24 h.

Conclusion

The appended hydroxyl substituents of the (imino)pyridine ligands Hpyph, Hpyet, and Hpypr behave differently in the reaction with $CuCl_2$ under the same conditions. In the case of the ethylene-based ligand Hpyet, the solid structure of **2** reveals a bidentate N,N binding with no Cu--OH interactions. Surprisingly, a slightly longer propyl analogue yielded a considerably different crystal structure for the dinuclear Cu(II) complex **3**, as a result of a nucleophilic addition of the appended propyl alcohol to the aldehyde group of 2-pyridinecarboxaldehyde. Despite the lack of X-ray data for the phenyl derivative **1**, the symmetrical dimeric structure similar to that of **2** was proposed based on FT-IR, PXRD, and ESR data. Activity comparisons of the catalyst system Cu(II) complex/Cu^0/TEMPO/Na_2CO_3 in water revealed that different coordination environments at the dinuclear copper centers in **2** and **3** do not have a significant impact on catalytic oxidation of benzyl alcohol. On the other hand, lower activities of **1** was contributed to the presence of the more electron-withdrawing phenylene groups in the ligand framework. In general, this work provides insights into different chemical behaviors of the appended hydroxyl groups based on slightly different ligand chain lengths. Lessons learned from the corresponding Cu coordination and subsequent catalytic alcohol oxidation activities in water of these complexes should be applicable to other metal complexes of related hydroxyl-containing ligand systems.

View Article Online
DOI: 10.1039/C7NJ03113K

Acknowledgements

This research is funded by the Thailand Research Fund (Grant No. RSA6080082) The authors also gratefully acknowledge Center for Innovation in Chemistry (PERCH-CIC), Faculty of Science, Mahidol University and Mahidol University under the National Research Universities Initiative. A.J. also appreciates financial assistance from Science Achievement Scholarship of Thailand (SAST).

Supplementary Materials. Characterization data for all new compounds reported in this work, crystallographic data contained in a CIF file of the Cu(II) complexes **2** (CCDC 1564878) and **3** (CCDC 1564879) are available free of charge *via* the Internet at xxxxx.

References

1. O. Das and T. K. Paine, in *Transition metal catalysis in aerobic alcohol oxidation*, eds. F. Cardona and C. Parmeggiani, The Royal Society of Chemistry, 2015, DOI: 10.1039/9781782621652-00040, ch. 2, pp. 40-69.
2. M. F. Sammelhack, C. R. Schmid, D. A. Cortes and C. S. Chou, *J. Am. Chem. Soc.*, 1984, **106**, 3374-3376.
3. P. Gamez, I. W. C. E. Arends, J. Reedijk and R. A. Sheldon, *Chem. Commun.*, 2003, 2414-2415.
4. E. T. T. Kumpulainen and A. M. P. Koskinen, *Chem. Eur. J.*, 2009, **15**, 10901-10911.
5. J. M. Hoover, J. E. Steves and S. S. Stahl, *Nat. Protoc.*, 2012, **7**, 1161-1166.
6. P. Thongkam, S. Jindabot, S. Prabpai, P. Kongsaeree, T. Wititsuwannakul, P. Surawatanawong and P. Sangtrirutnugul, *RSC Adv.*, 2015, **5**, 55847-55855.
7. M. Kongkaew, K. Sitthisuwannakul, V. Nakarajouyphon, S. Pornsuwan, P. Kongsaeree and P. Sangtrirutnugul, *Dalton Trans.*, 2016, **45**, 16810-16819.
8. P. J. Figiel, A. Sibaouih, J. U. Ahmad, M. Nieger, M. T. Räisänen, M. Leskelä and T. Repo, *Adv. Synth. Catal.*, 2009, **351**, 2625-2632.
9. G. Zhang, X. Han, Y. Luan, Y. Wang, X. Wen, L. Xu, C. Ding and J. Gao, *RSC Adv.*, 2013, **3**, 19255-19258.
10. G. Zhang, Y. Z. Zhang, W.-F. Lo, J. Jiang, J. A. Golen and A. L. Rheingold, *Polyhedron*, 2016, **103**, 227-234.
11. B. H. Lipshutz, M. Hageman, J. C. Fennewald, R. Linstadt, E. Slack and K. Voigtritter, *Chem. Commun.*, 2014, **50**, 11378-11381.
12. J. A. D. Cooper, W. Smith, M. Bacila and H. Medina, *J. Biol. Chem.*, 1959, **234**, 445-448.
13. J. W. Whittaker, *Chem. Rev.*, 2003, **103**, 2347-2363.
14. P. Gamez, I. A. Koval and J. Reedijk, *Dalton Trans.*, 2004, 4079-4088.
15. M. E. Moustafa, P. D. Boyle and R. J. Puddephatt, *Chem. Commun.*, 2015, **51**, 10334-10336.

View Article Online
DOI: 10.1039/C7NJ03113K

16. K. A. Thompson, C. Kadwell, P. D. Boyle and R. J. Puddephatt, *J. Organomet. Chem.*, 2017, **829**, 22-30.
17. D. Sunirban, S. A. Maloor, S. Pal and S. Pal, *Cryst. Growth Des.*, 2006, **6**, 2013-2018.
18. S. Striegler and M. Dittel, *Inorg. Chem.*, 2005, **44**, 2728-2733.
19. A. W. Addison, T. N. Rao, J. Reedijk, J. v. Rijn and G. C. Verschoor, *J. Chem. Soc. Dalton Trans.*, 1984, 1349-1356.
20. M. Rodríguez, A. Llobet, M. Corbella, A. E. Martell and J. Reibenspies, *Inorg. Chem.*, 1999, **38**, 2328-2334.
21. C. P. Pradeep and S. K. Das, *Polyhedron*, 2009, **28**, 630-636.
22. G. S. Nyamato, S. O. Ojwach and M. P. Akerman, *Dalton Trans.*, 2016, **45**, 3407-3416.
23. C. P. Pradeep and S. K. Das, *Coord. Chem. Rev.*, 2013, **257**, 1699.
24. X. R. Bu, C. R. Jackson, D. V. Derveer, X. Z. You, Q. J. Meng and R. X. Wang, *Polyhedron*, 1997, **16**, 2991-3001.
25. M. S. Ray, R. Bhattacharya, S. Chaudhuri, L. Righi, G. Bocelli, G. Mukhopadhyay and A. Ghosh, *Polyhedron*, 2003, **22**, 617-624.
26. A. M. Arnaiz, A. Carbayo, J. V. Cuevas, V. Diez, G. García-Herbosa, R. González, A. Martínez and A. Muñoz, *Eur. J. Inorg. Chem.*, 2007, 4637-4644.
27. L. Bendahl, A. Hammershøi, D. K. Jensen, S. Larsen, A. Riisager, A. M. Sargeson and H. O. Sørensen, *J. Chem. Soc. Dalton Trans.*, 2002, 3054-3064.
28. T. Birkle, A. Carbayo, J. V. Cuevas, G. García-Herbosa and A. Muñoz, *Eur. J. Inorg. Chem.*, 2012, 2259-2266.
29. N. A. Bailey, D. E. Fenton, R. Moody, C. O. Rodriguez de Barbarin and I. N. Sciambarella, *J. Chem. Soc. Dalton Trans.*, 1987, 2519-1529.
30. K. R. J. Thomas, P. Tharmaraj and V. Chandrasekhar, *Polyhedron*, 1995, **14**, 977-982.
31. E. Garribba and G. Micera, *J. Chem. Ed.*, 2006, **83**, 1229-1232.
32. J. E. Steves and S. S. Stahl, *J. Am. Chem. Soc.*, 2013, **135**, 15742-15745.
33. S. Harrisson, P. Couvreur and J. Nicolas, *Macromolecules*, 2012, **45**, 7388-7396.
34. L.-M. Zhang and T. C. W. Mak, *J. Am. Chem. Soc.*, 2016, **138**, 2909-2912.
35. B. L. Ryland, S. D. McCann, T. C. Brunold and S. S. Stahl, *J. Am. Chem. Soc.*, 2014, **136**, 12166-12173.

View Article Online
DOI: 10.1039/C7NJ03113K

A table of content:

Effects of appended hydroxyl group's chain length from a series of (imino)pyridine ligands on copper coordination and copper-catalyzed aerobic oxidation of alcohols were investigated.